Effect of optimized aging processing on properties of the sintered Dy-doped Nd–Fe–B permanent magnet*

Wang Xiao-Li(王晓丽)[a)b)], Zhao Li-Na(赵利娜)[a)], Ding Kai-Hong(丁开鸿)[c)], Cui Sheng-Li(崔胜利)[c)], Sun Yong-Cong(孙永聪)[c)], and Li Mu-Sen(李木森)[a)†]

[a)] *Key Laboratory for Liquid-Solid Structural Evolution and Processing of Materials of Ministry of Education, Shandong University, Jinan* 250061, *China*

[b)] *Jiangsu University of Science and Technology Institute of Materials, Zhenjiang* 212003, *China*

[c)] *Yantai Shougang Magnetic Materials Inc., Yantai* 265500, *China*

(Received 22 September 2014; revised manuscript received 24 October 2014; published online 30 January 2015)

We investigate the effect of the optimized aging processing on magnetism and mechanical property of the sintered Dy-doped Nd–Fe–B permanent magnet. The experimental results show that the magnetism, especially intrinsic coercivity, of the optimized aged Dy-doped Nd–Fe–B magnet is more excellent than that of the sintered one, but the former's strength and hardness are lower than that of the latter. It was observed that the optimized aged Dy-doped Nd–Fe–B magnet have more uniform grain size, thinner (Nd, Dy)-rich boundary phase. By means of the EBSD technology, the number of larger angle grain boundaries in the optimized aged Dy-doped Nd–Fe–B magnet is more than that of the sintered one. The reasons for the increased intrinsic coercivity and decreased mechanical properties of the optimized aged Dy-doped Nd–Fe–B magnet are also discussed.

Keywords: Dy-doped Nd–Fe–B magnet, magnetism, strength, morphology

PACS: 75.50.Ww, 75.50.Vv, 67.80.dk, 71.20.Eh **DOI:** 10.1088/1674-1056/24/3/037506

1. Introduction

It is well known that the sintered (Nd, Dy)–Fe–B magnets have high corrosion resistance and a high intrinsic coercive force,[1] and thus have been widely used in many fields of aviation and navigation, electronic information technology, green energy, transportation, communications, health, etc. In view of the development trend, the application areas of permanent magnetic material with desirable properties will continue to expand. In the future, they will be used under more and more harsh conditions, such as the motor vehicle with a speed over 10 kr/min. As a result, severe working conditions raise higher requirements to the strength and toughness to prevent the cracking of the served magnet.[2] Therefore, the study on mechanical properties of sintered Nd–Fe–B alloy has attracted more attention in recent years.

Horton *et al.*[3,4] discussed the mechanical properties of the Nd–Fe–B magnet in different processing routes. Zhang *et al.*[5] studied the failure mechanism of sintered Nd–Fe–B magnets from the view of a fracture model and fracture mechanism as well as the effect of alloying on strength and toughness. The results showed that intercrystalline fracture is the main fracture model and cracks are elongated along the interface between the $Nd_2Fe_{14}B$ phase and Nd-rich phase. Rabinovich *et al.*[6] examined the strength, fracture toughness, Young's modulus, hardness, as well as the other physical properties of sintered Nd–Fe–B series with different compositions. The results revealed that the bending strength σ_{bb} measured with three-point-bend method of ternary NdFeB magnets is about 200–250 MPa and the fracture toughness K_{IC} with the single-edge-notched-bend (SENB) method is about 2.5–3.7 MPa·m$^{1/2}$. Jiang *et al.*[7,8] checked that the strength σ_{bb} of magnets could be improved to 400 MPa by Co element alloying, but K_{IC} (tested also by the SENB method) is even lower than that of the ternary NdFeB magnet. Liu *et al.*[9] reported a significant improvement of impact toughness by the compositional modification with Nd content variation and/or a small amount of Ti, Cu, and Nb addition. Li *et al.*[10] also presented the positive effect of proper Nd content in grain boundary phase on the mechanical properties of sintered Nd–Fe–B magnets by the dual-alloy sintered process. Liu *et al.*[11] examined the mechanical properties including bending strength (σ_{bb}) and fracture toughness of sintered Nd–Fe–B magnets with Dy, Co, Nb additions, and discussed the fracture mechanism.

However, there has been less work on the magnetism and mechanical property of Dy-doped Nd–Fe–B permanent magnet alloys in the literature. In this paper, the difference of the magnetic and mechanical properties between the sintered and the optimized aging processed Dy-doped Nd–Fe–B permanent magnets is compared and analyzed by means of the FESEM observation on the fracture and grain boundaries analysis by EBSD technology in order to provide a basis for the development of high-performance sintered Nd–Fe–B permanent magnets.

*Project supported by the Chinese National Major Special Project for the Rare Earth and Rare Metallic Materials (Grant No. (2012) 1743).

†Corresponding author. E-mail: msli@sdu.edu.cn

© 2015 Chinese Physical Society and IOP Publishing Ltd

2. Experimental details

2.1. Materials preparation and magnetic properties

The Dy-doped Nd–Fe–B magnets with the commercial serial number of N35TH was employed. The mass percentage of Dy of the Dy-doped Nd–Fe–B magnets was 3%–5%. The coercive force of the optimized aged Dy-doped Nd–Fe–B magnet with this composition is the best and its mechanical properties were studied. The samples were prepared by the standard powder metallurgy method using multiple alloy powders doped Dy–Fe alloy powders. After magnetic field alignment and pressing, the green compacts were sintered at 1050 °C for 2 h. After the sintering process, the two stages of aging heat treatments were employed. In order to find the most appropriate temperature, several aging treatments were applied for the sintered magnets by using an electric tube furnace under the condition of 10^{-3} Pa vacuum. In the first stage of the high-temperature aging, the aging temperatures were selected between 600 °C and 1050 °C with an interval of 50 °C for 2 h. In the second stage of the low-temperature aging, the aging temperatures were selected between 430 °C and 560 °C with an interval of 10 °C for 2 h. Then the optimized aging processing consists of 2 h first aging at 800–950 °C and 2 h second aging at 430–500 °C. All of the aged samples were cooled to room temperature slowly.

Magnetic measurements were performed with the NIM-2000 type magnetic measuring instrument made by National Institute of Metrology of China. The magnetic parameters such as intrinsic coercive force (H_{cj}), magnetic induction coercive force (H_{cb}), bending point (H_k), remanence (B_r), maximum energy product ($(BH)_{max}$), and the squareness can be obtained from the measured demagnetization curves.

2.2. Mechanical properties test

Bending strength tests were performed with an Instron 8502 servo-hydraulic fatigue testing system with the three-point bending. The three point bending was made in accordance with the GB/T 14452-93 procedure. The three-point bending specimen was fixed on a specifically designed jig for three-point bending tests in a fatigue testing machine. The test samples are the Dy-doped NdFeB magnets with the size of 5 mm × 5 mm × 35 mm. The span width is $L = 25.7$ mm. The loading rate is 0.3 mm/min. Examinations of the sintered and optimal aged Nd–Fe–B magnets were repeated five times and the average results are given because of larger random error. The bending strength is calculated via international standard BS EN ISO 3327:2009, [12]

$$R_{tr} = \frac{3PL}{2bh^2}, \tag{1}$$

where P is the load required to fracture the test specimen (N), L is the distance between supports (25.7 mm), b is the width of the test beam (5 mm), and h is the height of the test beam (5 mm). Surface preparation is an important variable and should be standardized to ensure that consistent results are obtained. Figure 1 is a schematic diagram of the three point bending test.

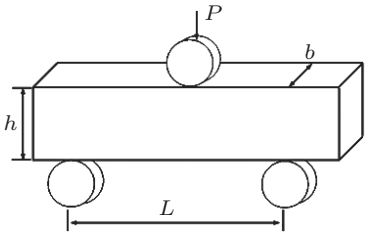


Fig. 1. Schematic diagram of the three point bending test (in unit of mm).

Compressive strength tests were performed on an SCHENCK TREBEL testing machine made in Germany in accordance with the GB/T 10424-12002 procedure. The test samples are the Dy-doped Nd–Fe–B magnets with the size of Φ10 mm×8 mm. The loading rate is 5 mm/min. A minimum number of five specimens were examined for each condition and the average results are given. Compressive strength is calculated by

$$\delta_s = \frac{4F}{\pi d^2}, \tag{2}$$

where F is the load required to fragment the test specimen (N), and d is the diameter of the samples.

Vickers-hardness tests were performed with a DV-1000 model of hardness tester under a test load of 2.94 N for 10 seconds. All the experiments were repeated at least ten times to characterize the dispersion of the experimental results.

2.3. Fracture and EBSD test

In this study, the fracture surface morphology was observed by a UC-70 model of thermal field emission scanning electron microscopy (TFESEM) made in Japan and the boundaries analysis was used by EBSD technology.

3. Results and discussion

3.1. Magnetic test

The main magnetic parameters such as intrinsic coercivity, remanence, and squareness of Dy-doped Nd–Fe–B magnets treated by the optimal aging process are measured. These values are also compared with that of the sintered Dy-doped Nd–Fe–B magnets. Figure 2 shows the demagnetization curves of the sintered and the optimal aged Dy-doped Nd–Fe–B magnets and Table 1 lists the main magnetic parameters of the two samples. The data in Table 1 and Fig. 2 show that compared with the sintered sample, the intrinsic coercivity, the energy product, and the remanence of the optimal aged Dy-doped magnets are all improved greatly. It is worth noting that the intrinsic coercivity, H_{cj}, is increased remarkably, from 19.912 kOe for the sintered magnet to 24.949 kOe for the optimal aged magnet. The H_{cj} is obviously increased by 25.3% after the optimized aging treatment.

Table 1. Comparison of magnetic properties between the sintered and the optimized aging processed Dy-doped magnets.

Sample	Sintered	Optimal aged
B_r/kGs	12.263	12.318
Hcb/kOe	11.851	12.105
H_{cj}/kOe	19.912	24.949
H_k/kOe	19.420	23.708
H_k/H_{cj}	0.975	0.950
$(BH)_{max}$/MGsOe	36.032	37.152

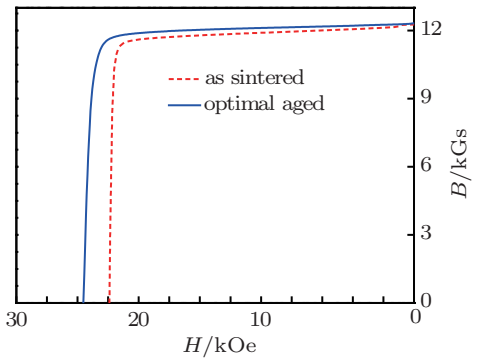


Fig. 2. (color online) Demagnetization loops of the sintered (a) and the optimal aged Dy-doped magnets (b).

3.2. Mechanical properties

The bending strength, compressive strength, and Vickers hardness of the sintered magnets are 381.27 MPa, 1299.58 MPa, and 613.2 HV, respectively, while the corresponding values of the optimized aging processed magnets are 298.16 MPa, 1021.87 MPa, and 561.8 HV. After optimized aging, the bending strength of the Dy-doped Nd–Fe–B permanent magnets falls by 21.8%, the compressive strength by 21.4%, and Vickers hardness by 8%, respectively. However, the bending strength of the Dy-doped Nd–Fe–B magnets is higher than that of the Dy-free Nd–Fe–B magnets as reported in Ref. [6]. This result is in agreement with that of Liu.[11] Mechanical properties of the Dy-doped Nd–Fe–B magnets are shown in Table 2. From the magnetism and mechanical properties, it can be seen that after the optimal aging processing, the intrinsic coercivity of the sintered Dy-doped Nd–Fe–B permanent magnets is obviously increased, but the compressive strength, bending strength, and hardness decrease. In order to study the property change of the Dy-doped Nd–Fe–B permanent magnets, the microstructure observation and fracture analysis are performed.

Table 2. Comparison of mechanical properties between the sintered and the optimized aging processed Dy-doped Nd–Fe–B magnets.

Sample	Bending strength/MPa	Compressive strength/MPa	Vickers hardness/HV
Sintered	381.27	1299.58	613.2
Optimized aging processed	298.16	1021.87	561.8

3.3. Microstructure observation and fracture analysis

Figures 3(a) and 3(c) show the fractographs of the sintered Dy-doped Nd–Fe–B magnet and figures 3(b) and 3(d) show the fractographs of the optimized aging processed Dy-doped Nd–Fe–B magnet. As shown in Figs. 3(a) and 3(b), after the optimized aging treatment, the grain size of the Dy-doped Nd–Fe–B permanent magnets becomes uniform; simultaneously Nd-rich phase that is mainly distributed along the grain boundary becomes thinner, as shown in Fig. 3(c) and 3(d). Therefore, there are three reasons responsible for the increase of H_{cj}. Firstly, H_{cj} is related to the anisotropy field H_A of the main phase in the magnets. The anisotropy field of $Dy_2Fe_{14}B$ ($H_A = 15.0$ T) is much higher than that of $Nd_2Fe_{14}B$ ($H_A = 7.6$ T).[13] Secondly, H_{cj} is closely related to the grain size of the magnets, and the small grains are in favor of high H_{cj}.[14] Thirdly, the grain boundary (GB) phase plays an important role in determining the H_{cj}. The thinner film of the Nd-rich phase has been formed in the GB during optimized aging processing. This kind of GB can effectively separate the magnetic grains, weaken the static magnetic coupling demagnetization effect, and improve the H_{cj} of magnet.

Intercrystalline fracture is the main fracture model, which can be concluded from the micrograph of the fracture surface as shown in Fig. 3. The thin film Nd-rich phase uniformly distributed around the matrix grain plays a significant role in increasing the coercive force, but it is also the main reason for the intergranular fracture of the Dy-doped Nd–Fe–B magnet since it has a much lower hardness than that of the matrix phase. Therefore, a crack easily expands along the grain boundary in the Nd-rich phase.[15] The grain boundary strength of magnets with heterogeneous grain size is always higher owing to bigger grain boundary sliding resistance than that of the magnets with uniform grain size. At the same time, the grain boundary strength is also enhanced by the Nd-rich phase because the Nd-rich phase is ductile phase and always forms large particles in the crystal, while the grain boundary strength becomes smaller when the Nd-rich phase in the magnets forms mainly in the thin grain boundary. Therefore, the sliding resistance along the grain boundary of the main crystal phase $(Nd, Dy)_2Fe_{14}B$ particle is larger and the grain boundary strength is higher; while for the magnet after aging treatment, the sliding resistance along the grain boundary of the main crystal phase particles decreases and the grain boundary strength is lower. From the backscattered images and image analysis system for quantitative analysis of the Nd rich phase, it is found that the proportion of the Nd-rich phase in the sintered magnets is 16.28%, while the proportion of the optimized aging processed magnets is only 11.51%. Zeng *et al.*[16] found that cracks are elongated in the intercrystalline Nd-rich phase since this phase is weak. Liu *et al.*[9,17] showed

that the strength of the Nd-rich phase is lower than that of the $Nd_2Fe_{14}B$ phase, but the toughness of the former is better. Therefore, the mechanical strength and hardness of the sintered Dy-doped Nd–Fe–B magnets are higher than that of the optimized aging treated one.

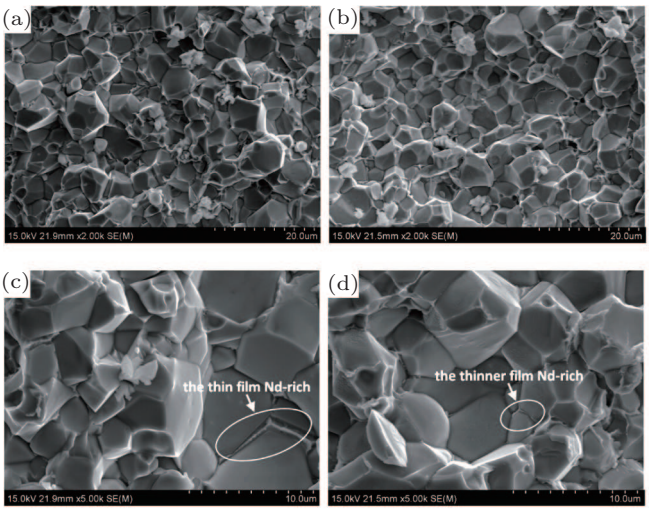


Fig. 3. Fracture morphology of (a, c) sintered and (b, d) optimized aging processed Dy-doped magnets.

3.4. EBSD analysis

EBSD orientation data are represented by the Euler angle. Misorientation (including shaft and angle of misorientation) can be computed by two orientations. The grain boundary which has a 15 degrees or bigger misorientation is a large-angle grain boundary, otherwise it is a small-angle grain boundary. A small-angle grain boundary is a representation of one status in the interior of a grain, while a large-angle boundary corresponds to two different grains. Differences in distribution and types of large and small angle grain boundary caused by different treatment processes influence the alloy performance to a certain extent. Figure 4 shows the grain boundary analysis results by the EBSD of the sintered and optimized aging processed magnets. The small-angle boundary of about 5°–15° is shown as red, while the large-angle boundary exceeding 15° is shown as yellow. After two stages of aging treatment, the amount of small-angle grain boundary decreases, while that of the large-angle grain boundary increases. The increase in the large-angle grain boundary is conducive to the liquidity of the Nd-rich phase in the grain boundary, so that the lamellar structures are formed, which improves the coercivity of the magnets. On the other hand, the increase of large-angle grain boundary reduces the sliding resistance of the main crystalline phase of the $(Nd, Dy)_2Fe_{14}B$ particles along the grain boundaries. Therefore, the optimized aging Dy-doped Nd–Fe–B magnet's magnetic properties are better than that of the sintered ones, but the bending strength, compressive strength, and Vickers hardness of the former are lower than those of the latter.

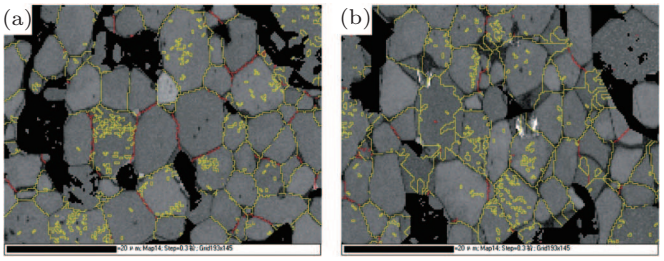


Fig. 4. (color online) EBSD diagrams of (a) sintered and (b) optimized aging processed Dy-doped magnets.

4. Conclusion

The experimental results show that the magnetism, especially intrinsic coercivity, of the optimized aged Dy-doped Nd–Fe–B magnet is more excellent than that of the sintered one and the H_{cj} value of the former is increased by 25.3% compared with the latter. The strength and hardness of the optimized aged Dy-doped Nd–Fe–B magnet are lower than those of the sintered one. The bending strength, compressive strength, and the Vickers hardness of the former fall by 21.8%, 21.4%, and 8%, respectively. It is observed by TFE-SEM that the optimized aged Dy-doped Nd–Fe–B magnet has more uniform main crystal grain size and thinner (Nd, Dy)-rich boundary phase which are the main reason for improving its magnetism. By means of the EBSD technology, the number of larger angle grain boundaries in the optimized aged Dy-doped Nd–Fe–B magnet is much more than that of the sintered one so as to lower the strength and hardness of the optimized aged Dy-doped Nd–Fe–B magnet due to the sliding resistance along the grain boundary falling.

References

[1] Yu L Q, Wen Y H and Yan M 2004 *J. Magn. Magn. Mater.* **283** 353
[2] Ceng Z P 1996 *Rare Metal Mat. Eng.* **25** 18
[3] Horton J A, Wright J L and Herchenroeder J W 1986 *IEEE Trans. Mag.* **32** 4374
[4] Horton J A, Herchenroeder J W, Wright J L and Easton D S 1996 *Mater. Trans. JIM* **37** 860
[5] Zhang H and Yang X P 2006 *Proceeding of* 19*th International Workshop on Rare Earth Permanent Magnets & Their Applications*, Beijing, China
[6] Rabinovich Y M, Sergeev V V and Maystrenko A D 1996 *Intermetallics* **4** 641
[7] Jiang J H, Zeng Z P and Wu J S 2000 *J. Magn. Magn. Mater.* **214** 61
[8] Jiang J H, Zeng Z P and Wu J S 2001 *Intermetallics* **9** 269
[9] Liu S, Cao D and Leese R 2002 *Proceedings of the* 17*th International Workshop on Rare Earth Magnets and Their Applications*, Newark DE, USA
[10] Li A H, Li W and Dong S Z 2003 *J. Magn. Magn. Mater.* **265** 331
[11] Liu W and Wu J S 2008 *J. Alloy. Compd.* **458** 292
[12] BS EN ISO 3327. 2009 *Hard Metals - Determination of Transverse Rupture Strength. European Committee for Standardization*, Brussels
[13] Kronmüller H, Durst K D and Sagawa M 1988 *J. Magn. Magn. Mater.* **74** 291
[14] Zhou S Z and Dong Q F 2004 *Super Permanent Magnets-Permanent Magnetic Material of Rare-earth and Iron system* (Beijing: Metallurgy Industry Publishing)
[15] Sun X X, Bao X Q and Gao X X 2009 *J. Trans. Mater. Heat Treat.* **29** 31
[16] Zeng Z P 1996 *J. Rare Metal Mat. Eng.* **25** 18
[17] Li J F and Liu S 2004 *Proceeding of* 18*th International Workshop on High Performance Magnets and Their Applications*, Annecy, France